Theor Chem Acc (2010) 127:681–687
DOI 10.1007/s00214-010-0778-7

REGULAR ARTICLE

Factors influencing the binding of a potassium cation to a polyethylene glycol type podand in liquid–liquid extraction—a molecular dynamics study

Mário Valente · Sérgio Filipe Sousa · A. L. Magalhães · Cristina Freire

Received: 18 May 2010 / Accepted: 18 June 2010 / Published online: 6 July 2010

Abstract The potassium cation complexation using a potentially octadentate polyethylene glycol type podand (*1,2-bis-{2-[2-(2-metoxy-etoxi)-etoxy]-etoxy}-benzene*, hereafter *b33*) in an organic (dichloromethane) phase is studied by molecular dynamics (MD). Specifically, the influence of the picrate (*2,4,6-trinitrophenolate*) anion and of water molecules on the complexation of K^+ by *b33* is analyzed. The results point out to a strong influence of the picrate anion on the K^+ complexation as this anion competes with the podand for the cation, reducing its mean denticity (here defined as the number of strong interactions established between the cation and the podand oxygen atoms, e.g. with inter-atomic K^+–O distances less than 4 Å) from 8 to *c.a.* 7. The presence of a water micro-droplet (comprising twelve water molecules) exerts a stronger effect on the podand mean denticity, reducing it to *c.a.* 5. The simultaneous presence of a picrate anion and the water micro-droplet dramatically reduces the podand denticity toward the cation to *c.a.* 2. When present, the water molecules effectively bind K^+, and it is the hydrated cation that is complexed: the podand becomes the second coordination sphere by establishing hydrogen bonds with the first coordination sphere of water molecules. In some simulations, π-stacking between the picrate anion and the podand aromatic ring was observed, as was, in others, the formation of "water fingers".

Keywords Molecular dynamics simulations · Alkali metal cation extraction · Ethylene-glycol type podands

1 Introduction

Liquid–liquid extraction is an important separative technique in such fields as analytical and industrial chemistry, where it frequently achieves very good efficacy/cost ratios, and a good understanding of the extraction mechanism may be of great value to the design of more effective extraction agents [1].

The alkali metal cation extraction from an aqueous phase to an organic phase is fundamentally dependent on the complexation between the cation, initially present in the aqueous phase, and an extraction agent typically present in the organic phase [2]. The liquid–liquid extraction of alkali metal cations by polyethers has been assumed to take place mainly (1) in the bulk organic phase [3] implying the migration of the cation (or the cation/anion pair) to the organic phase where it would bind to the extraction agent, (2) in the bulk aqueous phase [4] considering the migration of the extraction agent to the aqueous phase where the binding to the cation would happen followed by a migration of the complex to the organic phase, or (3) at the interface [5].

In a previous paper [6], we described how alkali metal cation complexes with *b33* (Fig. 1) are highly unstable in water, supporting the above-mentioned hypothesis of complexation in the bulk organic phase for these systems. As some water molecules are surely dragged to the organic

Electronic supplementary material The online version of this article (doi:10.1007/s00214-010-0778-7) contains supplementary material, which is available to authorized users.

M. Valente · S. F. Sousa · A. L. Magalhães (✉) · C. Freire (✉)
REQUIMTE/Departamento de Química e Bioquímica,
Faculdade de Ciências da Universidade do Porto,
Rua Campo Alegre s/n, 4169-007 Porto, Portugal
e-mail: almagalh@fc.up.pt

C. Freire
e-mail: acfreire@fc.up.pt

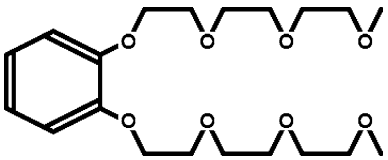

Fig. 1 Schematic representation of the podand *b33*

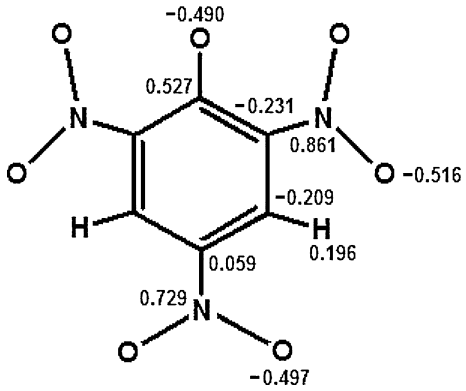

Fig. 2 Schematic representation of the picrate anion and the corresponding atomic charges used in its parameterization

phase during the extraction process [7], we wish to clarify in what way the presence of water molecules and of the most commonly used counter-ion in extraction experiments (the picrate anion) may influence the stability of the K^+ complex with *b33* in bulk dichloromethane.

As long as some care is taken [8], molecular dynamics (MD) has shown a good phenomenological validity in particular in systems where no heavy electronic rearrangements (e.g. due to bond breaking or bond forming) happen and is currently the method of choice to model systems as ours, not only because it allows the explicit inclusion of hundreds of solvent molecules (comprising thousands of atoms), but also because they are extremely fluxional and, as such, not adequate to a high level quantum calculation. It is noteworthy that alkali metal cation complexation by crown-ethers was one of the first problems to be studied by MD [9, 10], and most published work in this area has been on them [9–15] or on spherands [16–22], with only a few studies involving cryptands [5, 15] or podands [5, 23].

2 Methods

The molecular dynamics simulations were performed using the AMBER 9 [24] software package. The podand molecule and the picrate anion molecule were parameterized as previously described [6] using the Antechamber [25] module of AMBER in agreement with the typical premises followed in the general amber force field (GAFF) [26]. The GAUSSIAN 03 package [27] was used to perform a quantum mechanical calculation at the HF/6-31G* level of theory in order to get the ESP Merz–Kollman charges (4 layers, 6 points per unit area) on the picrate anion molecule (Fig. 2).

The van der Waals parameters used for the alkali cations were derived from the work of Åqvist [28], while dichloromethane was accounted for using the molecular mechanics parameters of Fox and Kollman [29]. For water, the well-known TIP3P model [30] was used.

The starting structure used for the complex consisted of a central K^+ cation embraced by the open arms of the *b33* podand molecule. As the solubility of water on dichloromethane is 0.24% (m/m) at 20 °C [31], which corresponds to about 11.3 water molecules per 1,000 dichloromethane molecules, we considered twelve water molecules in the simulations involving the hydration of the solute; the water molecules were added to the starting structure of the complex, also surrounding the central cation. For the simulations involving a picrate anion, the corresponding molecule was positioned above the K^+ cation and parallel to the complex. The orthogonal simulation cells consisted of the starting structures immersed in dichloromethane molecules to a minimum distance of 20 Å (all comprising c.a. 5,000 atoms).

All calculations were performed with the SANDER module of AMBER 9. Minimizations were performed by applying the steepest descent minimization method for ten thousand steps followed by an equal number of steps using the conjugate gradient minimization method. Equilibrations were performed sequentially in two stages: first the systems were allowed to heat from 0 to 300 K in fifty thousand steps (with a step time of 1 fs) using temperature control (Langevin dynamics with 1 ps^{-1} collision frequency), at constant volume (no pressure controls were applied). In the second equilibration step, the system was allowed to run for two hundred thousand steps (with the same time step) at 300 K, using the same temperature control conditions, at constant (isotropic) pressure, with a pressure relaxation time of 2 ps, in order to achieve the proper final density. To avoid changes on the complexes during the equilibration steps, the movements of all solutes were heavily restrained at their initial structures, using a force constant of 100 kcal mol^{-1} $Å^{-2}$.

The production run consisted of two million steps (corresponding to 2.0 ns) at constant (isotropic) pressure with a pressure relaxation time of 2 ps, using the same temperature control as above. During the production, MD runs information was extracted at a 200-step frequency, generating 10,000 frames. Throughout all minimization, equilibration and production steps a cut-off value of 12 Å was used.

As already mentioned, the systems under study are extremely fluxional, and good phase-space coverage is

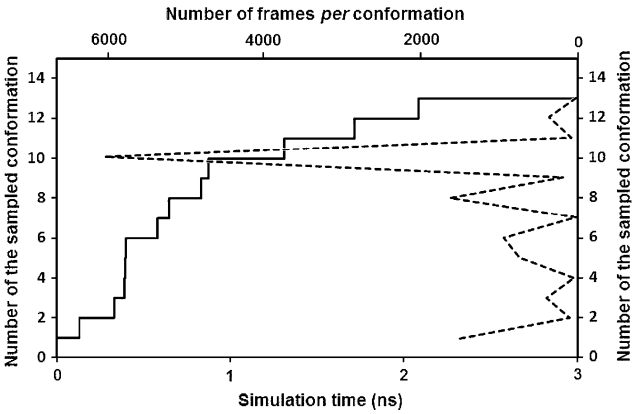

Fig. 3 Cumulative number of sampled conformations for *b33* (*solid line*), and number of frames *per* conformation (*dashed line*), as a function of the simulation time

Table 1 Percentage of the total simulation time ($\%_{t.s.t.}$) found for each podand denticity

Denticity	$\%_{t.s.t.}$			
	[K *b33*]$^+$	[K *b33* Pic]	[K *b33*]$^+$ + 12 H_2O	[K *b33* Pic] + 12 H_2O
0	0.0	0.0	26.1	71.2
1	0.0	0.0	8.0	9.9
2	0.0	0.0	6.7	12.8
3	0.0	0.0	8.6	4.9
4	0.0	0.4	13.0	1.1
5	0.0	3.1	15.9	0.1
6	0.4	28.0	16.8	0.0
7	6.6	39.8	4.1	0.0
8	93.0	28.7	0.8	0.0

expected in the total simulation time chosen (2.0 ns) [6]. Nonetheless, as a test on the space-phase coverage, we extended the simulation time of the least fluxional system, comprising a K^+/*b33* complex in dichloromethane, up to 3.0 ns.

Using the common definition [6, 33] for the $g+$ (60 ± 60°), $g-$ (−60 ± 60°) and t (180 ± 60°) dihedral angle arrangements and considering only the podand aliphatic OC–CO dihedral angles, the resulting trajectory was analyzed for the cumulative number of sampled conformations (each comprising six dihedral angle arrangements—Fig. 3) as a function of the simulation time (Fig. 3, solid line) and as a function of the number of sampled conformations (Fig. 3, dashed line).

As the OC–CO dihedral angles practically only adopt either $g+$ or $g-$ arrangements (see Sect. 3.2), the number of possible conformations (as defined earlier) for this podand is $2^6 = 64$, but by grouping the symmetrically equivalent ones, this number reduces to 36. The total number of conformations found in the extended simulation time of 3.0 ns was 13 and in the working simulation time of 2.0 ns the number of conformations found was 12. The number of frames found for the most frequently sampled conformation (number 10) was 6,036, but the thirteenth conformation (the one not encompassed in the 2.0-ns simulation time) was only sampled once. These results support the validity of the chosen simulation time.

3 Results and discussion

3.1 Potassium complexation

The percentage of the total simulation time found for each podand denticity (Table 1) indicates that the denticity is highly dependent on the close presence of either a picrate anion or of water molecules, as they compete effectively with the podand to establish strong interactions with the cation. The most common podand denticity in the absence of all but solvent (dichloromethane) molecules is 8 (for about 93.0% of the total simulation time, hereafter $\%_{t.s.t.}$), meaning that mostly all the eight potentially donor oxygen atoms present in the podand establish strong interactions with the cation, with a mean K^+–O_{podand} distance of 2.90 ± 0.06 Å.

In the close presence of a picrate anion, the podand denticity reduces to *c.a.* 7 (28.0$\%_{t.s.t.}$ for six, 39.8$\%_{t.s.t.}$ for seven and 28.7$\%_{t.s.t.}$ for eight interactions, with a combined duration of 96.5$\%_{t.s.t.}$). Due to steric effects, the picrate partially detaches the cation from the direct interaction with the podand oxygen atoms, reducing its effective denticity. The mean K^+–O_{podand} distance (considering only the strongly interacting oxygen atoms) is now 2.99 ± 0.08 Å.

In the presence of highly mobile, strongly competing water molecules, the podand is completely unbound to the cation for 26.1$\%_{t.s.t.}$. When bonded, its denticity is reduced to *c.a.* 5 (13.0$\%_{t.s.t.}$ for four, 15.9$\%_{t.s.t.}$ for five, and 16.8$\%_{t.s.t.}$ for six interactions, with a combined duration of 45.7$\%_{t.s.t.}$), with a mean K^+–O_{podand} distance (considering only the strongly interacting oxygen atoms) of 3.09 ± 0.05 Å.

In the combined presence of a picrate anion and of water molecules, the podand is completely unbound to the cation for most of the simulation time (71.2$\%_{t.s.t.}$), but when bonded the mean denticity is reduced to *c.a.* 2 (9.9$\%_{t.s.t.}$ for one and 12.8$\%_{t.s.t.}$ for two interactions, with a combined duration of 22.7$\%_{t.s.t}$). The mean K^+–O_{podand} distance (considering only the strongly interacting oxygen atoms) is now 3.22 ± 0.11 Å.

The picrate anion is naturally able to compete with the podand for the cation. The mean denticity found by the picrate anion, in the absence of water molecules, was 1.83 (with a mean K^+–$O_{picrate}$ distance of 2.93 ± 0.07 Å). The

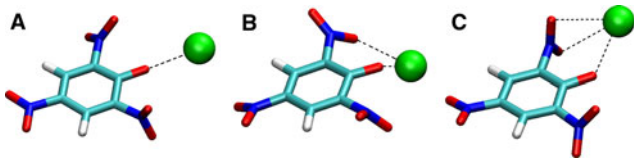

Fig. 4 Typical structures for the picrate anion acting as a (**a**) mono-, (**b**) bi- and (**c**) tridentate ligand toward the K^+ cation

picrate anion was in the free form for 10.5%$_{t.s.t.}$, with a mean life time[1] of 6.62 ps (except for one longer time of 80.60 ps), and acted as a mono-dentate ligand for 20.0%$_{t.s.t.}$, with a mean life time of 5.84 ps, (Fig. 4a), as bi-dentate ligand for 65.0%$_{t.s.t.}$, with a mean life time of 6.14 ps, (Fig. 4b), and as tri-dentate ligand for 4.5%$_{t.s.t.}$, with a mean life time of 1.47 ps, (Fig. 4c), meaning that, in the absence of water, and for a total time of 89.5%$_{t.s.t.}$, this anion forms a close contact ion pair with the K^+ cation.

In the presence of water molecules, the picrate anion mean denticity is reduced to 1.53 (with a mean K^+–$O_{picrate}$ distance of 3.18 ± 0.12 Å). The anion was in the free form for 36.0%$_{t.s.t.}$, with a mean life time of 5.16 ps (except for two longer times of c.a. 90 ps each), and acted as a mono-dentate ligand for 31.5%$_{t.s.t.}$, with a mean life time of 2.67 ps, as bi-dentate ligand for 31.5%$_{t.s.t.}$, with a mean life time of 2.86 ps, and only as transiently as a tri-dentate ligand, meaning that for 64.0%$_{t.s.t.}$ the picrate anion forms a close contact ion pair with the K^+ cation.

As previously stated, in the presence of water molecules the podand is able to act mostly as a tetra- to hexa-dentate ligand, thus partially occupying the K^+ cation coordination sphere, leaving less space for more water molecules to coordinate. As can be seen from the percentage of time, the cation is surrounded by "*n*" water molecules at distances of less than 4 Å (Table 2), the most frequent number of water molecules surrounding the K^+ cation ranges from two to six in the absence of picrate and four to seven in its presence. This increase is due to the partial detachment of the cation from the podand caused by the picrate anion. This allows for a greater number of water molecules to surround the cation.

This analysis is corroborated by the radial distribution functions, $g(r)$, built for the twelve water oxygen atoms considered (Table 3). In the absence of picrate, the water oxygen atoms appear somewhat more dispersed than in the presence of the anion, in particular from the seventh to the twelfth water molecule.

Typically, water molecules acted cooperatively in binding the K^+ cation to the podand, by surrounding the cation as a first coordination sphere that is itself bound by hydrogen bonding to the podand (Fig. 5).

Occasionally, water molecules are kept near the podand by binding to the K^+ cation that in turn is bound to the podand oxygen atoms. A good example of this is the frame presented in Fig. 6, where two sets of water molecules (one with five, the other with three molecules) form independent "water fingers" that bind to the cation and simultaneously stretch into the organic phase.

Similar phenomena were reported for the 1,2-dimethoxyethane [33], 18-crown-6 [34–36], calixarene [37], and 222-cryptand [22] systems in water. A good experimental example is the X-ray structure of a binary hydrate between 18-crown-6 and six water molecules [38].

Table 2 Percentage of the total simulation time (%$_{t.s.t.}$) in which the K^+ cation is surrounded by "*n*" water molecules at distances of less than 4 Å

Number of waters	%$_{t.s.t.}$	
	[K *b33*]$^+$ + 12 H_2O	[K *b33* Pic] + 12 H_2O
0	0.0	0.0
1	2.7	0.1
2	18.7	1.2
3	18.3	4.7
4	16.4	22.3
5	21.3	33.0
6	13.5	23.7
7	6.8	11.1
8	1.8	3.4
9	0.3	0.6
10	0.1	0.0
11	0.0	0.0
12	0.0	0.0

Table 3 K^+–O_W mean distances (Å) for the twelve water molecules, from integration of the $g(r)$ function for the whole simulation time

Water	[K *b33*]$^+$ + 12 H_2O	[K *b33* Pic] + 12 H_2O
1st	4.4	5.0
2nd	5.6	6.0
3rd	6.5	6.7
4th	7.3	7.6
5th	8.1	8.3
6th	9.0	9.0
7th	10.3	9.8
8th	12.1	10.7
9th	14.6	12.0
10th	20.1	13.3
11th	24.8	16.6
12th	31.9	25.5

[1] Only sequences of five or more frames (corresponding to 1 ps) where the picrate anion kept a constant denticity were considered when computing the mean life times present, so as to eliminate the spurious highly transient states.

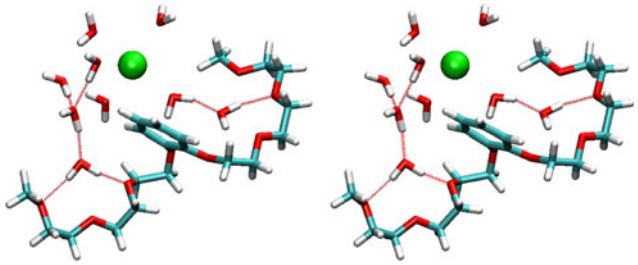

Fig. 5 Stereo-view [32] of a frame where six water molecules directly bound to the K^+ cation (*solid lines*) are themselves bound to the podand by cooperative hydrogen bridges (*dashed lines*)

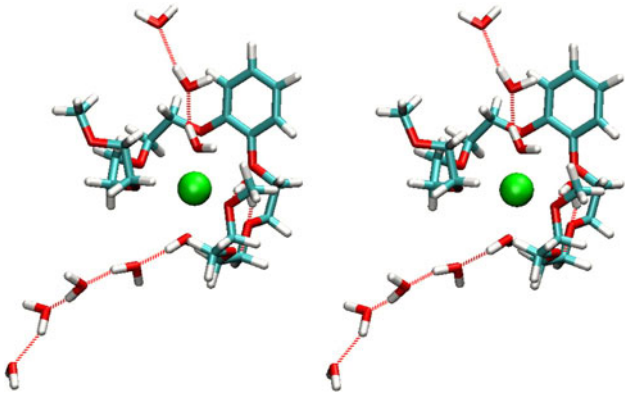

Fig. 6 Stereo-view of a frame where two sets of water molecules, directly bound to the K^+ cation, form two "water chains" by hydrogen bonding (*fine lines*)

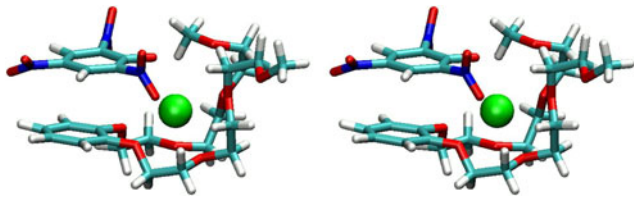

Fig. 7 Stereo-view of a frame where π-stacking between the picrate anion and the aromatic ring of the podand is observed

We also observed the occurrence of π-stacking between the picrate anion and the benzene ring of the podand for five times (with a mean lifetime of 170 ps) during the 2.0 ns of simulation for the [K *b33* Pic] system in dichloromethane (Fig. 7). The mean inter-aromatic ring distance found was 4.0 ± 0.5 Å, and the picrate anion mostly acted as a mono-dentate ligand toward the K^+ cation while interacting by π-stacking with the podand aromatic ring. Counterpoise-corrected calculations on the arbitrarily chosen π-stacked structure depicted in Fig. 7 (using the GAUSSIAN 03 package at the HF/6-31G* level of theory) yielded a repulsive interaction between the picrate anion and the podand molecule of 28 kcal/mol.

The π-stacking between two picrate anions in water has been found experimentally and studied by MD [39] and by Troxler et al. [40], where it was found that two picrate anions remained stacked in water, for the whole duration of the simulation (400 ps) with a mean inter-aromatic ring distance of 3.9 ± 0.4 Å and a calculated (PMF) dimerization free energy of 41–45 kcal/mol.

3.2 Podand conformational analysis

The podand conformation at each moment, as defined previously, may be defined as a sequence of arrangements ($g-$, $g+$ or t) for each dihedral angle involving the atoms pertaining to its chain [6]. It is clear from the percentage of time determined for each arrangement found for all skeletal dihedral angles (Table 4) that the CO–CC (and the CC–OC) dihedral angles adopt preferentially t arrangements and that the OC–CO dihedral angles present almost exclusively $g+$ or $g-$ arrangements.

If the phase-space is adequately covered during a simulation, one would expect to see a symmetrical distribution of the dihedral angle arrangement durations in both arms (centered on the dihedral angle number 11), as the K^+ cation is able to octa-coordinate to the *b33* podand [6]. Deviations from the distribution symmetry are expected if the podand oxygen atoms are involved in strong interactions that are able to stabilize a given conformation over others. The most unsymmetrical distribution is found for the $[K\ b33]^+$ system, indicating the presence of the above-mentioned strong conformation-stabilizing interactions. The strength of these interactions is reduced in the presence of any competing species and, as a result, the dihedral angle distribution becomes more symmetrical. In fact, the distributions of the other systems are quite symmetrical due to the perturbing competition posed by the picrate anion or by the water molecules. The presence of these molecules destabilizes the strong interaction between the K^+ cation and the podand oxygen atoms, thus increasing the fluxional character of the podand arms and allowing for a better coverage of the dihedral angle phase-space.

The mean OC–CO dihedral angle values increase with the increase in perturbation on the direct K^+ cation to podand binding. The value found for the $[K\ b33]^+$ system (65 ± 2°) is lower than the one found for the [K *b33* Pic] system (69 ± 5°), which in turn is lower than those found for the $[K\ b33]^+ + 12\ H_2O$ system (74 ± 1°) and for the [K *b33* Pic] + 12 H_2O system (79 ± 1°). The mean dihedral angle values found for the two latter systems are very close to those reported for the free podand in bulk water (73.1 ± 1.3°) and in bulk dichloromethane (80.7 ± 1.0°), respectively [6]. For the $[K\ b33]^+ + 12\ H_2O$ system, the partial removal of the K^+ cation form direct interaction with the podand oxygen atoms by water molecules that

Table 4 Percentage of the total simulation time ($\%_{t.s.t.}$) for each arrangement ($g-$, $g+$ or t) for the CO–CC, OC–CO and CC–OC dihedral angles of the podand arms

Dihedral number	Dihedral type	$\%_{t.s.t.}$											
		[K *b33*]$^+$			[K *b33* Pic]			[K *b33*]$^+$ + 12 H_2O			[K *b33* Pic] + 12 H_2O		
		$g-$	$g+$	t	$g-$	$g+$	T	$g-$	$g+$	T	$g-$	$g+$	T
1	CO–CC	4.3	5.4	**90.3**	9.5	2.6	**87.9**	4.1	3.5	**92.4**	5.3	10.9	**83.8**
2	***OC–CO***	34.7	**65.2**	0.1	**51.7**	46.1	2.2	**65.3**	32.4	2.3	27.9	**69.2**	2.9
3	CC–OC	2.6	9.4	**88.0**	0.9	5.8	**93.3**	16.7	3.8	**79.5**	6.9	11.0	**82.1**
4	CO–CC	6.1	0.2	**99.7**	7.0	0.6	**92.4**	1.1	3.5	**95.4**	5.6	6.5	**87.9**
5	***OC–CO***	**55.6**	44.4	0.0	**51.0**	48.9	0.1	**72.3**	25.9	1.8	30.1	**67.5**	2.4
6	CC–OC	0.0	12.9	**87.1**	1.3	36.3	**61.4**	2.7	2.3	**95.0**	5.8	4.0	**90.2**
7	CO–CC	10.7	0.1	**89.2**	16.4	0.1	**83.5**	2.7	13.0	**84.3**	2.0	11.7	**86.3**
8	***OC–CO***	31.1	**68.9**	0.0	18.9	**81.1**	0.0	25.4	**72.9**	1.7	**66.6**	28.8	4.6
9	CC–OC	0.0	**62.8**	37.2	0.4	26.4	**73.2**	2.6	17.7	**79.7**	7.7	21.7	**70.6**
10	CO–CC	18.5	1.3	**80.2**	0.4	30.4	**69.2**	5.0	33.8	**61.2**	15.1	19.0	**65.9**
11	***OC–CO***	**50.2**	49.8	0.0	49.4	**50.6**	0.0	48.3	**51.7**	0.0	49.7	**50.3**	0.0
12	CC–OC	21.5	0.3	**78.2**	32.1	0.3	**67.6**	16.1	11.3	**72.6**	20.4	10.9	**68.7**
13	CO–CC	0.0	**82.8**	17.2	2.1	21.2	**76.7**	0.6	11.5	**87.9**	0.2	13.2	**86.6**
14	***OC–CO***	0.0	**100.0**	0.0	48.0	**51.5**	0.5	25.6	**74.0**	0.4	30.4	**65.2**	4.4
15	CC–OC	0.3	0.3	**99.4**	13.6	10.6	**75.8**	0.5	16.5	**83.0**	6.4	9.3	**84.3**
16	CO–CC	0.1	1.5	**98.4**	14.4	14.2	**71.4**	3.0	2.8	**94.2**	5.1	9.2	**85.7**
17	***OC–CO***	**96.5**	3.4	0.1	42.7	**56.0**	1.3	40.4	**58.9**	0.7	**68.0**	27.2	4.8
18	CC–OC	2.3	3.0	**94.7**	1.6	9.8	**88.6**	4.7	1.3	**94.0**	8.2	3.4	**88.4**
19	CO–CC	8.1	4.6	**87.3**	9.8	26.5	**63.7**	9.2	3.0	**87.8**	10.1	10.6	**97.3**
20	***OC–CO***	8.7	**91.0**	0.3	**68.5**	26.4	5.1	**65.0**	33.4	1.6	**49.0**	48.8	2.2
21	CC–OC	0.4	8.0	**91.6**	9.8	4.9	**85.3**	6.1	4.1	**89.8**	9.9	5.7	**84.4**

may be, themselves, complexed to the podand via hydrogen bonds results in a system where the podand is nearly hydrated as in bulk water. The combined action of the picrate anion and the water molecules on the [K *b33* Pic] + 12 H_2O system almost results in a removal of the K^+ cation from the podand in what could be seen as a synergic effect, thus increasing the OC–CO dihedral angle to almost the value found for free podand in dichloromethane.

4 Conclusions

We found that the presence of water molecules dramatically reduces the denticity of the podand and may in fact reduce its selectivity based on the number of cation–oxygen podand strong interactions. The picrate anion also seems to compete for the cation and is able to strongly reduce the podand denticity, as it effectively acts as a mono/bi-dentate ligand. It tends to form a π-stacked structure with the podand and, simultaneously, a stable tight ion pair with the K^+ cation in pure dichloromethane but, in the presence of water molecules, the tight ion pair mean life time is heavily reduced, as the cation tends to become hydrated. The podand is able to bind to the hydrated cation by means of hydrogen bonding, forming a second coordination sphere around the K^+ cation, but probably reducing the podand selectivity.

Double solvent box steered MD studies are under way in order to give new insights into the process of crossing the water–dichloromethane interface.

References

1. Moyer BA, Bonnesen PV, Custelcean R, Delmau LH, Hay BP (2005) Kem Ind 54:65–87
2. Frensdorff HK (1971) J Am Chem Soc 93:4684–4688
3. Cram DJ (1986) Angew Chem Int Ed Engl 25:1039–1057
4. Takeda Y, Endo K, Yoshiyama D, Watanabe K, Fukada N, Katsuta S (2007) J Molec Liquids 130:21–28
5. Nazarenko AY, Baulin VE, Lamb JD, Volkova TA, Varnek AA, Wipff G (1999) Ion Exch Membr 17:495–523
6. Valente M, Sousa SF, Magalhães AL, Freire C (2010) Journal of Molecular Structure: THEOCHEM 946:77–82
7. Fan W, Tsai R-S, Tayar NE, Carrupt P-A, Testa B (1994) J Phys Chem 98:329–333
8. van Gunsteren WF, Mark AE (1998) J Chem Physics 108:6109–6116

9. Bovill MJ, Chadwick DJ, Sutherland IO (1980) J Chem Soc Perkin II 1529–1543
10. Wipff G, Weiner P, Kollman P (1982) J Am Chem Soc 104:3249–3258
11. Grootenhuis PDJ, Kollman P (1989) J Am Chem Soc 111:2152–2158
12. Mazor MH, McCammon JA, Lybrand TP (1990) J Am Chem Soc 112:4411–4419
13. Wang J, Kollman P (1998) J Am Chem Soc 120:11106–11114
14. Vayssière P, Wipff G (2003) Phys Chem Chem Phys 5:2842–2850
15. Troxler L, Wipff G (1994) J Am Chem Soc 116:1468–1480
16. Kollman PA, Wipff G, Singh UC (1985) J Am Chem Soc 107:2212–2219
17. Grootenhuis PDJ, Kollmann PA, Groenen LC, Reinhoudt DN, Van Hummel GJ, Ugozzoli F, Andreetti GD (1990) J Am Chem Soc 112:4165–4176
18. Miyamoto S, Kollman PA (1992) J Am Chem Soc 114:3668–3674
19. Varnek A, Wipff G (1996) J Comput Chem 17:1520–1531
20. Thuéry P, Nierlich M, Lamare V, Dozol J-F, Asfari Z, Vicens J (1997) Supramol Chem 8:319–332
21. Sieffert N, Wipff G (2006) J Phys Chem B 110:19497–19506
22. Auffinger P, Wipff G (1991) J Am Chem Soc 113:5976–5988
23. Solov'ev VP, Baulin VE, Strakhova NN, Kazachenko VP, Belski VK, Varnek AA, Volkova TA, Wipff G (1998) J Chem Soc Perkin II 1489-1498
24. Case DA, Darden T, Cheatham T, Simmerling CL, Wang J, Duke RE, Luo R, Merz KM, Perlman DA, Crowley M, Walker RC, Zhang W, Wang B, Hayik S, Roitberg A, Seabra G, Wong KF, Paesani F, Wu X, Brozell S, Tsui V, Gohlke H, Yang L, Tan C, Mongan J, Hornak V, Cui G, Berosa P, Mathews DH, Schafmeister C, Ross WS, Kollman PA (2006), AMBER 9, University of California, San Francisco
25. Wang J, Wang W, Kollman PA, Case DA (2006) J Mol Graph Model 25:247–260
26. Wang J, Wolf RM, Caldwell JW, Kollman PA, Case DA (2004) J Comput Chem 25:1157–1174
27. Gaussian 03, Revision C.02, Frisch MJ, Trucks GW, Schlegel HB, Scuseria GE, Robb MA, Cheeseman JR, Montgomery JA Jr, Vreven T, Kudin KN, Burant JC, Millam JM, Iyengar SS, Tomasi J, Barone V, Mennucci B, Cossi M, Scalmani G, Rega N, Petersson GA, Nakatsuji H, Hada M, Ehara M, Toyota K, Fukuda R, Hasegawa J, Ishida M, Nakajima T, Honda Y, Kitao O, Nakai H, Klene M, Li X, Knox JE, Hratchian HP, Cross JB, Adamo C, Jaramillo J, Gomperts R, Stratmann RE, Yazyev O, Austin AJ, Cammi R, Pomelli C, Ochterski JW, Ayala PY, Morokuma K, Voth GA, Salvador P., Dannenberg JJ, Zakrzewski VG, Dapprich S, Daniels AD, Strain MC, Farkas O, Malick DK, Rabuck AD, Raghavachari K, Foresman JB, Ortiz JV, Cui Q, Baboul AG, Clifford S, Cioslowski J, Stefanov BB, Liu G, Liashenko A, Piskorz P, Komaromi I, Martin RL, Fox DJ, Keith T, Al-Laham MA, Peng CY, Nanayakkara A, Challacombe M, Gill PMW, Johnson B, Chen W, Wong MW, Gonzalez C, Pople JA, Gaussian, Inc., Wallingford CT, 2004
28. Åqvist J (1990) J Phys Chem 94:8021–8024
29. Fox T, Kollman PA (1998) J Phys Chem B 102:8070–8079
30. Jorgensen WL, Chandrasekhar J, Madura JD, Impey RW, Klein ML (1983) J Chem Phys 79:926–936
31. http://macro.lsu.edu/howto/solvents/Dichloromethane.htm (last accessed in June 2010)
32. Russel DW (1977) Stereo-viewing. Chem Brit 13:354
33. Straatsma TP, McCammon JA (1989) J Chem Phys 90:3300–3305
34. Straatsma TP, McCammon JA (1989) J Chem Phys 91:3631–3637
35. Ranghino G, Romano S, Lehn JM, Wipff G (1985) J Am Chem Soc 107:7873–7877
36. Ha YL, Chakraborty AK (1991) J Phys Chem 95:10781–10787
37. Lauterbach M, Engler E, Muzet N, Troxler L, Wipff G (1998) Phys Chem B 102:245–256
38. Mootz D, Albert A, Shaefgen S, Stäben D (1994) J Am Chem Soc 116:12045–12046
39. Harrowfield JM (1996) J Chem Soc Dalton Trans 3165-3171
40. Troxler L, Harrowfield JM, Wipff G (1998) J Phys Chem A 102:6821–6830